Covalently-Linked Hyaluronan Promotes Bone Formation around Ti Implants in a Rabbit Model

Marco Morra,[1] Clara Cassinelli,[1] Giovanna Cascardo,[1] Milena Fini,[2] Gianluca Giavaresi,[2] Roberto Giardino[2]

[1]Nobil Bio Ricerche, Str. S. Rocco 36, 14018 Villafranca d'Asti, Italy, [2]Experimental Surgery Laboratory, Institute Codivilla Putti, Rizzoli, Orthopaedic Institute, Bologna, Italy

Received 23 September 2006; accepted 18 September 2008
Published online 7 November 2008 in Wiley InterScience (www.interscience.wiley.com). DOI 10.1002/jor.20797

ABSTRACT: The goal of this study was the in vivo evaluation of nanoporous titanium (Ti) implants bearing a covalently linked surface hyaluronan (HA) layer. Implant surface topography and surface chemistry were previously evaluated by scanning electron micorscopy and X-ray photoelectron spectroscopy. Results showed that the surface modification process did not affect surface topography, yielding a homogeneously HA-coated nanotextured implant surface. In vivo evaluation of implants in both cortical and trabecular bone of rabbit femurs showed a significant improvement of both bone-to-implant contact and bone ingrowth at HA-bearing implant interfaces at 4 weeks. The improvement in osteointegration rate was particularly evident in the marrow-rich trabecular bone (bone-to-implant contact: control 22.5%; HA-coated 69.0%, $p < 0.01$). Mechanical testing (push-out test) and evaluation of interfacial bone microhardness confirmed a faster bone maturation around HA-coated implants (Bone Maturation Index: control 79.1%; HA-coated 90.6%, $p < 0.05$). Suggestions based on the biochemical role of HA are presented to account for the observed behavior. © 2008 Orthopaedic Research Society. Published by Wiley Periodicals, Inc. J Orthop Res 27:657–663, 2009

Keywords: bone implants; osteointegration; hyaluronan; biochemical modifcation of Ti surfaces

Titanium (Ti) implant devices are being widely used for a variety of indications in orthopedic and dental implantation surgery, and most of the various techniques in use are evidence-based and predictable. Interfacial interactions at the bone–implant interface are recognized as the key to osteointegration and an enormous literature on Ti surfaces and on approaches to the surface modification of Ti exists.[1–3] Still, Ti and its surface are actively investigated to address difficult clinical settings, that is, low bone density, as in the case of highly cancellous bone, or low vascularity, as in the case of primarily cortical bone, or insufficient quantity of bone (in terms of the width of the alveolar ridge) or poor bone stock as in the case of revision surgery. Moreover, new challenges for the future stemming from the increase of life expectancy are to be faced to reduce interfacial fibrous tissue formation especially in orthopedics,[4] and to accelerate initial healing times during osteointegration processes even in old, or, in general, patients with pathologic bone.[5]

Traditional approaches to surface modification of Ti are based on the control of surface topography,[3] on ceramic coatings,[6] and on physicochemical[7] or inorganic approaches.[8] Presently, a significant research effort is aimed at the biochemical modification of Ti surfaces (BMTiS), defined by Puleo and Nancy[9] as the immobilization of proteins, enzymes, or peptides for the purpose of inducing specific cell and tissue responses, using critical organic components of bone. BMTiS are generally based on surface modification by peptides, or Extra Cellular Matrix (ECM) proteins.[10] Beside proteins and peptides, Rammelt and coworkers have recently shown that a glycosaminoglycan (GAG), chondroitin sulphate (CS), coadsorbed with collagen, enhances the effects on bone remodelling at periimplant interfaces, underlying the role that ECM GAGs can play in osteointegration.[11,12]

Hyaluronan (HA) is a linear polysaccharide consisting of the repeating disaccharide unit N-acetyl-D-glucosamine-D-glucuronate, linked by β1–4 and β1–3 linkages.[13–16] Significant interest on HA as a biomaterial and in biomaterial surface modification exists,[14–18] and several literature reports indicate its potential interest for BMTiS: it has been known since the 1950s that considerable HA is synthesized in the early stages of callus formation during the repair of fractured long bones.[19] Iwata and Urist[20] found that large amounts of HA were secreted when implants of decalcified bone remineralized as bone. Bernard and coworkers[21] presented studies aimed at developing "a foundation for the use of HA as a superior carrier for osteotropic substrates, even as HA acts to enhance osteogenesis due to its own molecular structure." Their in vitro studies using fetal calvarial cells and bone marrow osteogenic stem cells show that osteogenesis in vitro is significantly enhanced by HA 30–160 kDa, while high Mw HA (550–1300 kDa) shows a weak inhibitory effect compared to the control. Zou and coworkers[22] reported that 800 kDa HA added to bone marrow stromal cells cultured in vitro accelerates cell proliferation, increases ALP activity and osteocalcin gene expression, and that HA interacts with BMP-2 to generate direct and specific cellular effects. Ito and coworkers[23] have shown that locally applied 900 kDa HA has a positive effect in bone ingrowth in Ti fiber mesh implant in rats. According to Cho,[24] HA shows a positive effect in early bone consolidation in distraction osteogenesis. Stancikova[25] reported that HA oral intake increases bone density of ovariectomised rats. Finally, HA-based scaffolds aid in the regeneration of cartilage and bone defects in tissue engeneering applications, and the hypothesis of an active role played by local HA

Correspondence to: Marco Morra (T: +39 0141 942446; F: +390141 941956; E-mail: mmorra@nobilbio.it)

delivery upon scaffold degradation has been also suggested.[26]

Based on the previous arguments, the present study was performed to evaluate in vivo the effect of HA covalently linked to Ti implants on bone regeneration. Uncoated and HA-coated Ti screws were implanted in both cortical and trabecular bone of rabbits and evaluated at 4 weeks by means of histologic, histomorphometric, and mechanical tests. The hypothesis of the present investigation was that a HA-coated Ti surface would offer some benefits in terms of screw osteointegration thanks to its chemistry, which could increase bone healing and maturation around implants.

MATERIALS AND METHODS

Sample Preparation

Commercially Pure Ti implant screws (cpTi, grade 2), 10×1.8 mm, thread pitch 0.6 mm, were subjected to electrochemical treatment to obtain a nanoporous surface topography. Screws were specifically manufactured for this study. HA coupling was obtained by cyanoborohydride-promoted covalent linking of periodate-treated HA to surface amino groups introduced on the Ti surface by plasma deposition.[18] For these studies, 800-kDa HA from bacterial fermentation (Lifecore, Chaska, MN) was used. Implants were Ethylene Oxide sterilized before implantation surgery.

Surface Characterization

X-ray photoelectron sectroscopy (XPS) was performed with a Perkin-Elmer (Norwalk, CT) PHI 5400 ESCA system. The instrument is equipped with a Mg X-ray source, operated at 14 kV and 250 W. Quantification of elements was accomplished using the software and sensitivity factors supplied by the manufacturer.

Surface topography of Ti and HATi samples was evaluated by scanning electron microscopy (SEM), using a LEO 420 SEM (LEO Electron Microscopy Ltd, Cambridge, UK). Relevant instrumental parameters are reported on the micrographs. No preparation was performed on the samples before analysis. Surface porosity and mean pore size were evaluated by image analysis, using the ImageJ 1.34 software (Wayne Rasband, National Institute of Health, Bethesda, MD http://rsb.info.nih.gov/ij).

In Vivo Studies

The entire in vivo study was performed following European and Italian Law on animal experimentation. The experimental protocol was approved by the Scientific Technical and Ethical Committees of the Rizzoli Orthopaedic Institute (Bologna, Italy) and sent to the Italian Ministry of Health. A prehoc power analysis at 80% power, $p < 0.05$, was performed, and it was determined that five rabbits in each group were necessary to detect a change of 30% in the bone-to-implant contact and bone ingrowth data when comparing HATi and Ti implants. Adult skeletally mature male rabbits weighting 4.100 ± 0.250 kg were used (Charles River, Calco, Lecco, Italy). Rabbits were acclimated for 10 days maintained in single cages at a T of $20 \pm 0.5^{\circ}$C, humidity rate of $55 \pm 10\%$ and water and food ad libitum (Mucedola, Settimo Milanese, Milan, Italy). Implants were placed in sterile surgical conditions. General anesthesia was induced with an i.m. injection of 44 mg/kg ketamine (Ketavet 100, Farmaceutici Gellini SpA, Aprilia Lt, Italy) and 3 mg/kg xylazine (Rompun Bayer AG, Leverkusen, Germany), and assisted ventilation (O_2:1 L/min; N_2O: 0.4 L/min; isofluorane: 2.5–3%). The surgical wounds were sutured in two layers. In the postoperative period the animals were checked daily. Antibiotic therapy (cefazolin, 100 mg/kg) was administered preoperatively, immediately after surgery and after 24 h. Analgesics (metamizole chloride, 50 mg/kg) were prescribed in the immediate postoperative period. The health of the animals was evaluated during the entire study by a veterinarian. At the end of the experimental time (4 weeks) the animals were sacrificed by pharmacological euthanasia under general anesthesia with intravenous administration of Tanax (Hoechst, Frankfurt am Main, Germany), the femurs were removed, stripped of soft tissues, and prepared for subsequent analyses.

Bone Implantation

Five rabbits were used for cortical bone implantation. The femur middiaphyses was exposed and two holes with a 1.8-mm diameter were drilled at low speed and under continuous saline irrigation in the cortical bone of the right and left femurs. Control uncoated Ti screws were transversally implanted in the left femurs of all rabbits, while HATi screws were positioned in the right femurs, up to a total of 10 cortical implants for each material. Five specimens for each material were used to evaluate the mechanically strength of the bone–implant fixation whereas the other five specimens for each material were used to evaluate bone-to-implant contact, bone ingrowth, and newly formed bone hardness by means of histologic, histomorphometric, and microhardness analyses.

Five rabbits were used for trabecular bone implantation. A 2-cm skin incision was made on the lateral aspect of both distal femurs. Holes were manually drilled in both femoral epiphyses in stages with a 1-mm drill that was subsequently expanded with a 1.8-mm drill. Control uncoated Ti screws were transversally implanted in the right femurs of all rabbits, while HATi screws were positioned in the left femurs, up to a total of five implants for each type of screws. Five specimens for each material were used to evaluate bone-to-implant contact and bone ingrowth by means of histologic and histomorphometric analyses.

Push-Out Force Evaluation

The push-out test was carried out by placing the diaphyseal femoral segments on a support jig with a clearance hole of 3.5 mm in diameter using a MTS apparatus (Sintech-1/M, MTS Adamel Lhomargy, Ivry sur Seine, France). A force was applied to the implant from the medullar side at a constant crosshead speed of 2 mm/min, which was pushed out of its bony bed. The maximum push-out force (F_{max}), that is, the peak force resulting in the detachment of the bone (coating)–implant system and corresponding to screw holding power was measured and calculated. After the push-out tests, the samples collected for each surface treatment were fixed and dehydrated, then observed with SEM (J840A, Jeol Tokyo, Japan) in secondary electrons mode to examine the failure mode at the bone–implant interface.

Histology and Histomorphometry

Half of the femoral cortical bone ($n = 5$) and all the femoral trabecular bone ($n = 5$) segments containing the implant were fixed in 4% buffered paraformaldehyde and then processed for embedding in epoxy resin (Struers Co. Copenhagen, Denmark). Blocks were sectioned along a plane parallel to

the long axis of the implanted screws. A series of sections of 200 ± 10 μm in thickness, were obtained with a Leica 1600 diamond saw microtome (Leica SpA, Milan, Italy). Then, sections were thinned to a thickness of 30 ± 10 μm and stained with fast green and acid fucsin. A total of three sections were analyzed for each specimen by using a transmission and polarized light Axioskop Microscope (Carl Zeiss GmbH, Jena, Germany) and a computerized image analysis system with Kontron KS 300 software (Kontron Electronic GmbH, Eiching bei Munchen, Germany). Measurements were taken semi-automatically by two experienced blinded investigators at a magnification of 12.5×. The following parameters were measured: (1) bone-to-implant contact or Affinity Index (AI, %): the length of bone directly opposed to the implant without the presence of a fibrous membrane divided by the total length of the bone–implant interface multiplied by 100. (2) Bone ingrowth (BI, %): bone area between the screw and the line connecting the thread crests divided by the total screw thread area expressed as percentage.

Microhardness

After samples preparation for histology and histomorphometry, the same resin-embedded blocks containing the implanted screws in cortical bone were used to measure bone hardness by means of an indentation test (Microhardness VMHT 30, Leica, Wien, Austria). After polishing, the smooth surface obtained was observed under the microscope and clearly showed the bone–material interface and the other areas to be examined. Microhardness measurements were taken tangentially to the interface with a Vickers indenter applied to the bone at a load of 0.05 kgf and dwell time of 5 s. The Vickers hardness degree (HV) was calculated by dividing the indentation force by the surface of the imprint observed at the microscope. The average value for each sample was calculated on a mean of 10 at two sites: (1) in the newly formed bone, within 200 μm from the implant surface and in the inner area in which the threads of the screw engage ($HV_{200\mu m}$); (2) outside the threads in the preexisting host bone not affected by implantation surgery, at 1000 μm from a line connecting the top of the threads ($HV_{1000\mu m}$). The bone maturation index (BMI) was calculated by dividing $HV_{200\mu m}$ by $HV_{1000\mu m}$ multiplied by 100.

Statistical Analysis

Statistical analysis was performed using SPSS v.12.1 software (SPSS Inc., Chicago, IL). After testing data for normal distribution and homogeneity of the variance, the nonparametric Wilcoxon signed-rank test, followed by the Monte Carlo methods to compute one-sided probability, were used to highlight significant differences between coated and uncoated screws. Data are reported as median and standard error of the mean (SE) at a significant level of $p < 0.05$ (one-tailed).

RESULTS

Surface Characterization by SEM and XPS

Representative SEM images of control Ti (a) and HATi (b) samples are shown in Figure 1 (15,000×). Images show the typical topography of anodically treated Ti above electric breakdown.[27] Pores look homogeneously distributed on the implant surface, image analysis yields average pore diameter of 260 ± 180 nm. The general appearance of the HATi surface is very similar to that of control Ti, and no significant difference of average pore diameter is detected. Thus, SEM analysis suggests that the process of HA coupling does not affect the original nanoporous surface topography; as expected, plasma deposition yields conformal coatings,[28] HA linking to the aminated surface is self-limited to interfacial coupling of a monomolecular layer,[18] that is to a fraction of a nanometer in the high vacuum environment of the SEM.

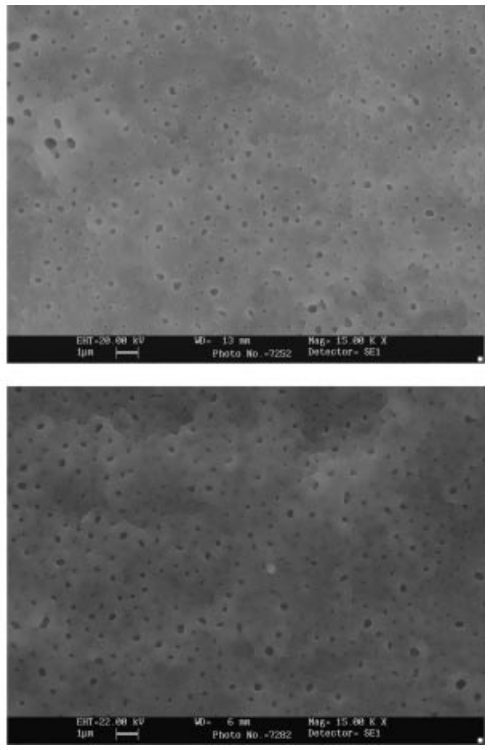

Figure 1. SEM micrographs of (a) Ti, 15k x; (b) HATi, 15k x.

Contrary to topography analysis, evaluation of surface chemistry by XPS yields very different results between the two set of samples (Table 1). The Ti sample shows, beside O, Ti, C, and N expected on every Ti implant surface, and Cl, also a common finding,[29,30] a large amount of P and the small, but significant, amount of S. These elements are due to the anodizing treatment, performed in a phosphate solution containing also sulphuric acid.[27] From a quantitative point of view, the detected figures, in particular, the C/Ti and O/C ratio are in general agreement with those expected on "clean" Ti surfaces.[2,29,30] Stoichiometry detected on HATi surfaces is completely different from that of Ti, despite the identical surface topography. Table 1 yields quantitative values in general agreement with those reported for HA coupled surfaces, albeit obtained using a different coupling process.[31,32] The detected figures indicate a fairly uniform HA coverage, as discussed in previous works.[31,32]

In Vivo Studies

All animals tolerated surgery well and survived the postsurgical period without any complications. When dissecting the femurs, the implants were checked and

Table 1. Surface Composition, as Detected by XPS Analysis, of Ti and HATi Samples (Data Are Expressed as % at)

Sample	O	C	N	Ti	P	Other (<1%)
Ti	39.5	35.4	1.3	12.7	8.2	Cl, S, Si
HATi	24.4	65.9	7.7	0.3	—	Si, Cl

neither macroscopic mal-positioning nor signs of infection were observed. Histology showed mature cortical or trabecular bone grown inside the screw threads in the absence of fibrous tissue at the bone–biomaterial interface in both Ti and HATi implants (Figs. 2 and 3). A higher amount of bone inside the screw threads and in contact with the surface of HATi implants could be observed. Both AI and BI parameters were higher on HATi implants compared to Ti, as showed in Table 2. Significant increases in AI and BI for HATi implants in trabecular bone in comparison to Ti implants were found. Statistical analysis of cortical bone parameters showed that, although the difference of percent increase of AI was significant at the $p < 0.05$ level, differences between BI values were not, albeit marginally ($p = 0.063$).

A significant higher value (25%) of maximum push out force (N) was found in HATi implant (median = 232.2, SE = 18.4) in comparison to Ti (median = 185.3, SE = 10.7). The SEM micrographs of cortical bone specimens after the push-out test revealed that bone failure occurred at the bone–implant interface. The preexisting host bone measured at 1000 μm from the bone–implant interface was not influenced by the different surface treatments, as expected. Periimplant bone microhardness data around HATi were higher than those around Ti, suggesting that there was not only more bone, as shown by histomorphometry, but that newly formed bone at the HATi implant interface was also more mature and mineralized compared to regrown bone in the proximity of the Ti surface. In particular, BMI (%) results of HATi (median = 90.6, SE = 1.0) were significantly ($p < 0.05$) higher than that of Ti (median = 79.1, SE = 1.0).

DISCUSSION

The aim of the present study was to evaluate whether a HA coating had a positive effect on the osteointegration of Ti implants. Results of the present work can be summarized as follows: (1) covalent linking of HA to nanoporous Ti implant surfaces allows to keep the original nanotextured topography while superimposing

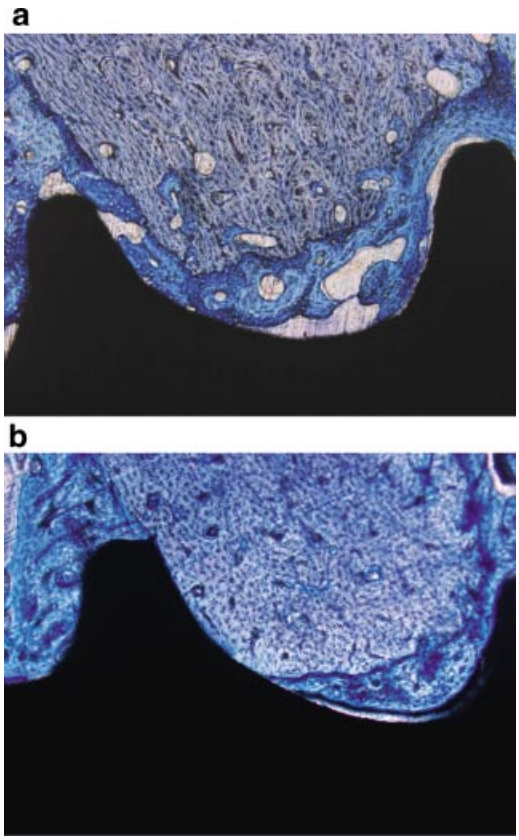

Figure 2. Examples of histological sections obtained from 4-week implants in rabbit femur cortical bone (original magnification ×10): a: Ti; b: HATi. [Color figure can be viewed in the online issue, which is available at http://www.interscience.wiley.com]

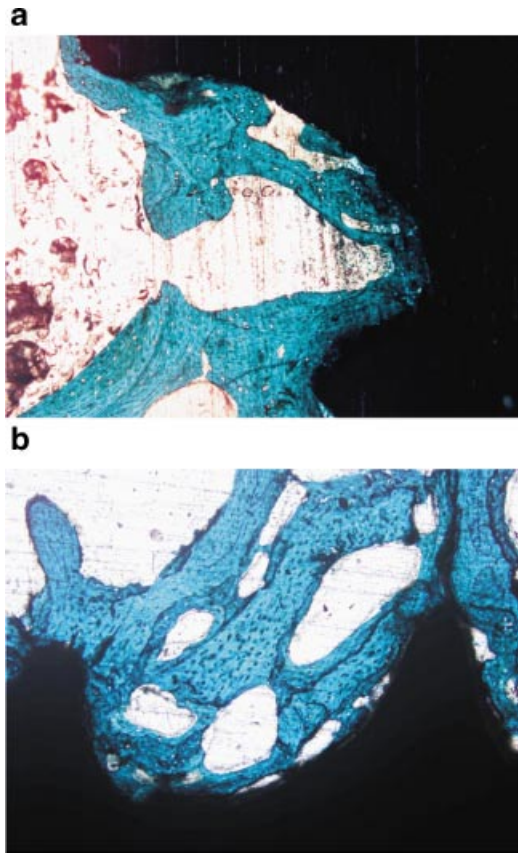

Figure 3. Examples of histological sections obtained from 4-week implants in rabbit femur trabecular bone (original magnfciation ×10): a: Ti; b: HATi. [Color figure can be viewed in the online issue, which is available at http://www.interscience.wiley.com]

Table 2. Histomorphometric results for Ti and HATi Implanted in Cortical and Trabecular Bone at 4 Weeks ($n = 5$)

		Cortical Bone		Trabecular Bone	
Implant		AI (%)	BI(%)	AI (%)	BI(%)
Ti	Median	55.0	84.5	22.5	30.3
	SEM	5.2	3.3	5.8	5.1
	(Min–Max)	(42.7–66.9)	(70.1–88.8)	(16.1–47.4)	(23.9–52.2)
HATi	Median	69.7*	91.0	69.0**	56.3*
	SEM	2.9	0.7	5.8	3.4
	(Min–Max)	(62.3–80.3)	(89.7–93.7)	(45.4–80.7)	(41.9–59.5)

AI = Affinity Index; BI = bone ingrowth.
Wilcoxon signed rank test: *$p < 0.05$; **$p < 0.01$.

the HA chemistry; (2) the HA coating significantly increased bone contact, bone ingrowth, implant mechanical fixation and bone maturation as demonstrated by in vivo studies in rabbit. All together, in vivo evidences pointed consistently in the direction of enhanced, or faster, bone regeneration at the HATi interface compared to the Ti interface.

A higher percentage of bone-to-implant contact and bone ingrowth does not necessarily relate to a proper mechanical fixation of implants. Because this could be due to the lower maturity and maturation of the newly formed bone at the interface,[33] microhardness test and BMI were measured. Bone microhardness analysis is a nondestructive technique that enables the comparative study of bone hardness variations at different distances from the interface that influence implant mechanical performaces.[34] In particular, some authors found correlation between microhardness and variables such as volume fraction of mineral, Young's modulus, yield stress, and calcium content, bone mineralization, and collagen fiber orientation.[35] Besides the bone hardness measured in the regrown bone (HV_{200}) and that measured in the preexisting host bone (HV_{1000}), we used the percentage of their ratio (HV_{200}/HV_{1000}) defined as BMI, which gives information about the possible influence of surface treatments on the process of bone maturation[35] obviously considering its preexisting host bone. In our study discrepancies between histomorphometric data and mechanical fixation were not observed, and mechanical results on implant fixation paralleled the histomorphometric data on biological osteointegration. This is because the higher amount of bone regrown around HATi implants was also mature and well mineralized.

The influence of HA coating on biological osteointegration was more evident in trabecular bone than in cortical bone. These data are in agreement with the ones of our and other authors' previous researcher in which it was observed that trabecular and cortical bone respond differently to the chemistry of implant surface when studying hydroxyapatite-coated Ti implants in vivo.[5,36] It is hypothesized that the effect of bioactive surfaces on tissue morphogenesis and vascularization, cell migration, and differentiation are more evident in a biologically superior tissue as trabecular bone is in comparison with cortical bone.[37]

Our interest was to investigate the effect of HA covalently linked to Ti implants on the early phases of the osseointegration processes. On the basis of other studies in rabbits,[38,39] it was of special interest to demonstrate also a significant higher osseointegration of HATi at a short time after surgery. Certainly, if other experimental times had been added the bone response around HATi implants could have been more completely investigated. Other authors found that the bone-to-implant contact of a HA gel coated hydroxyapatite surface did not significantly changed from 2 to 4 weeks together with a similar osteointegration rate in HA and hydroxyapatite-coated Ti alloy at 4 weeks and a higher mechanical fixation of HA gel coated hydroxyapatite surfaces than the uncoated one at 1, 2, and 4 weeks.[33]

Concerning the mechanism(s) that leads to enhanced bone response at HA interfaces, literature suggests few speculations. Carboxylates are natural sites for complexation of calcium ions, and the role of HA could just be that of provider of a highly carboxylate interface, that could act as nucleation sites for deposition of inorganic bone components. In 1904, Pfaundler[40] hypothesized that calcium binding was an important step during the calcification of the bone and that some unknown component of the bone was responsible. It was later discovered that GAGs play an important role, in particular, sulfated GAGs inhibit mineral growth: in fact, the concentration and size of constituent proteoglycans decrease when resting cartilage transitions into calcified cartilage during endochondral osteogenesis.[41] Although the formation of hydroxyapatite is inhibited by the charge density of sulfated GAGs, HA not only enhances hydroxyapatite crystal proliferation and growth, but it can even promote too much mineralization.[42–44] Mechanisms more directly related to the HA molecular structure exist as well: beside the works quoted in the Introduction,[18–25] it is worthy to underline that HA is a prominent extracellular matrix component during bone morphogenesis.[45,46] HA is found whenever there is need for rapid cell proliferation, repair, and regeneration. During an early stage of osteogenesis, when only undifferentiated mesenchymal cells are found, HA

reaches peak levels.[20] Quoting from Bernard "in terms of its correlation with wound healing mechanisms and hard tissue development, HA can be thought as a 'primer' in cell regeneration."[21] In this respect, the very significant enhancement of histomorphometry parameters detected in experiments in trabecular bone, that is a rich source of mesenchymal cells with the ability to proliferate along the osteogenic pathway, is very relevant.

It must be noted that HA-coated surfaces are, in general, resistant to cell adhesion, due to their significant interfacial hydration, as reported in the literature.[32] Work performed in this lab confirms that, even in the present case, HA-coated Ti surfaces do not support osteoblast cell adhesion in cell culture tests in vitro. However, the interaction of HA with its receptors on cell surface is modulated by interactions with cytokines transitorily expressed on wound healing.[17] As an example, Lesley[47,48] has shown that preincubation of HA with TSG-6 (tumor necrosis factor-stimulated gene 6), a hyaladherin expressed at sites of inflammation, enhances or induces the binding of hyaluronan to cell surface CD44. For the very role HA plays in tissue repair,[13–16] the HA–cell interaction cannot be disjoined by the specific environment that evolves on wound healing.

CONCLUSIONS

In conclusion, results show, by a number of different tested parameters and in both cortical and trabecular bone, that covalently linked HA stimulates bone regeneration at the implant interface, in a 4-weeks rabbit model. Several speculations are presented, to account for the observed effect on the basis of existing literature and experimental evidence. Open questions still remain, among them: (1) is the observed effect specifically due to HA or every surface-linked hydrophilic, caboxylated polysaccharide will yield the same results? (2) Is HA the only GAG that works, or, as suggested by the literature,[9,10] other GAGs such as chondroitin sulfate would yield the same trend? (3) Is there an effect of HA molecular weight on periimplant bone formation, as suggested by the literature? Finally, a limitation of this study is that just one time point was considered to obtain information mainly on the possibility of accelerating an early osteointegration and bone healing. Experiments aimed at addressing these points are currently underway.

ACKNOWLEDGMENTS

This study was entirely founded by Nobil Bio Ricerche srl, as a part of internal development project. Two of the authors (M.M. and C.C.) own shares of Nobil Bio Ricerche.

REFERENCES

1. Davies JE editor. 1991. The bone–biomaterial interface. Toronto: University of Toronto Press.
2. Davies JE editor. 2000. Bone engineering. Toronto: Em Squared.
3. Brunette DM, Tengvall P, Textor M, et al. editors. 2001. Titanium in medicine. Berlin: Springer.
4. Elmengaard B, Bechtold JE, Soballe K. 2005. In vivo study of the effect of RGD treatment on bone ongrowth on press-fit titanium alloy implants. Biomaterials 26:3521–526.
5. Borsari V, Fini M, Giavaresi G, et al. 2007. Sandblasted titanium osteointegration in young, aged and ovariectomized sheep. Int J Artif Organs 30:163–172.
6. Borsari V, Fini M, Giavaresi G, et al. 2008. Osteointegration of titanium and hydroxyapatite rough surfaces in healthy and compromised cortical and trabecular bone: in vivo comparative study on young, aged, and estrogen-deficient sheep. J Orthop Res.
7. Rupp F, Scheideler L, Olshanska N, et al. 2006. Enhancing surface free energy and hydrophilicity through chemical modification of microstructured titanium implant surfaces. J Biomed Mater Res 76A:323–334.
8. Cooper LF, Zhou Y, Takebe J, et al. 2006. Fluoride modification effects on osteoblast behavior and bone formation at TiO2 grit-blasted c.p. titanium endosseous implants. Biomaterials 27:926–936.
9. Puleo DA, Nanci A. 1999. Understanding and controlling the bone-implant interface. Biomaterials 20:2311–2321.
10. Morra M. 2006. Biochemical modification of Ti surfaces: peptides and ECM proteins. Eur Cell Mater 12:1–15.
11. Rammelt S, Illert T, Schneiders W, et al. 2005. Coating of titanium implants with collagen, RGD peptides and chondroitin sulfate. ICBME Proc 12:2B–02.
12. Rammelt S, Illert T, Bierbaum S, et al. 2006. Coating of titanium implants with collagen, RGD peptide and chondoitin sulphate. Biomaterials 27:5561–5572.
13. Evered D, Whelan J editors. 1989. The biology of hyaluronan. Chichester: Wiley.
14. Laurent TC editor. 1998. The chemistry, biology and medical applications of hyaluronan and its derivatives. London:Portland Press Ltd.
15. Abatangelo G, Weigel PH editors. 2002. Redefining hyaluronan. Amsterdam: Elsevier.
16. Kennedy JF, Phillips GO, Williams PA, et al. editors. 2002. Hyaluronan. Cambridge, UK: Woddhead Publishing Limited.
17. Chen WYJ, Abatangelo G. 1999. Function of hyaluronan in wound repair. Wound Rep Reg 7:79–89.
18. Morra M. 2005. Engineering of biomaterials surfaces by hyaluronan. Biomacromolecules 6:1205–1223.
19. Maurer PH, Hudak SS. 1952. The isolation of hyaluronic acid from callus tissue of early healing. Arch Biochem Biophys 38: 49–53.
20. Iwata H, Urist MR. 1973. Hyaluronic acid production and removal during bone morphogenesis in implants of bone matrix in rats. Clin Orthop Rel Res 90:236–245.
21. Bernard GW, Pilloni A, Kang M, et al. 2000. Osteogenesis in vitro and in vivo with hyaluronan and bone morphogenetic protein-2. In Abatangelo G, Weigel PH, editors. Redefining hyaluronan. New York: Elsevier. p 215–231.
22. Zou X, Li H, Chen L, et al. 2004. Stimulation of porcine bone marrow stromal cells by hyaluronan, dexamethasone and rhBMP-2. Biomaterials 25:5375–5385.
23. Itoh S, Matubara M, Kawauchi T, et al. 2001. Enhancement of bone ingrowth in a titanium fiber mesh implant by rhBMP-2 and hyaluronic acid. J Mater Sci Mater Med 12: 575–581.
24. Cho BC, Park JW, Baik BS, et al. 2002. The role of hyaluronic acid, chitosan, and calcium sulfate and their combined effect on early bony consolidation in distraction osteogenesis of a canine model. J Craniofacial Surg 13:783–793.
25. Stancikova M, Svik K, Istok R, et al. 2004. The effects of hyaluronan on bone resorption and bone mineral density in a rat model of estrogen deficiency-induced osteopenia. Int J Tissue React 26:9–16.

26. Solchaga LA, Temenoff JS, Gao J, et al. 2005. Repair of osteochondral defects with hyaluronan- and polyester-based scaffolds. Osteoarthritis Cartilage 13:297–309.
27. Sul YT, Johansson CB, Jeong Y, et al. 2001. Oxidized implants and their influence on the bone response. J Mater Sci Mater Med 12:1025–1031.
28. Yasuda H. 1985. Plasma polymerization. Orlando, FL: Academic Press.
29. Kasemo B, Lausmaa J. 1986. Surface science aspects of inorganic biomaterials. CRC Crit Rev Biocomp 2:335–380.
30. Morra M, Cassinelli C, Bruzzone G, et al. 2003. Surface chemistry effects of topography modification of titanium dental implants surfaces: 1. Surface analysis. Int J Oral Maxillofacial Implants 18:40–45.
31. Morra M, Cassinelli C. 1998. Simple model for the XPS analysis of polysaccharide coated surfaces. Surf Interf Anal 26:742–746.
32. Morra M, Cassinelli C. 1999. Non-fouling properties of polysaccharide-coated surfaces. J Biomater Sci Polym Ed 10: 1107–1124.
33. Aebli N, Stich H, Schwalder P, et al. 2005. Effects of bone morphogenetic protein-2 and hyaluronic acid on the osseointegration of hydroxyapatite-coated implants: an experimental study in sheep. J Biomed Mater Res 73A:295–302.
34. Huja SS, Katona TR, Moore BK, et al. 1998. Microhardness and anisotropy of the vital osseous interface and endosseous implants supporting bone. J Orthop Res 16:54–60.
35. Aldini NN, Fini M, Giavaresi G, et al. 2004. Osteointegration of bioactive glass-coated and uncoated zirconia in osteopenic bone: an in vivo experimental study. J Biomed Mater Res 68A: 264–272.
36. Moroni A, Heikkila M, Magyar G, et al. 2001. Fixation strength and pin tract infection of hydroxyapatite-coated tapered pins. Clin Orthop 388:209–217.
37. Davies JE. 2003. Understanding peri-implant endosseous healing. J Dent Educ 67:932–949.
38. Morra M, Cassinelli C, Cascardo G, et al. 2003. Surface engineering of titanium by collagen immobilization. Surface characterization and in vitro and in vivo studies. Biomaterials 24:4639–4654.
39. Morra M, Cassinelli C, Cascardo G, et al. 2006. Collagen I-coated titanium surfaces: mesenchymal cell adhesion and in vivo evaluation in trabecular bone implants. J Biomed Mater Res 78A:449–458.
40. Pfaundler M. 1904. Uber die elemente der Gewebservkalkung und ihre Beziehung zur Rachitisfrage. Jarhb Kinderheilk 60:123–133.
41. Howell DS, Pita JC. 1976. Calcification of growth plate cartilage with special reference to studies on micropuncture fluids. Clin Orthop 118:208–229.
42. Chen CC, Boskey AL. 1985. Mechanisms of proteoglycan inhibition of hydroxyapatite growth. Calcif Tissue Int 37:395–400.
43. Boskey AL, Maresca M, Wikstrom B, et al. 1991. Hydroxyapatite formation in the presence of proteoglycans of reduced sulfate content: studies in the brachymorphic mouse. Calcif Tissue Int 49:389–393.
44. Boskey AL, Dick BL. 1991. Hyaluronan interactions with hydroxyapatite do not alter in vitro hydroxyapatite crystal proliferation and growth. Matrix 11:442–446.
45. Toole BP, Gross J. 1971. The extracellular matrix of the regenerating newt limb: synthesis and removal of hyaluronate prior to differentiation. Dev Biol 25:57–77.
46. Toole BP, Jackson G, Gross J. 1972. Hyaluronate in morphogenesis: inhibition of chondrogenesis in vitro. Proc Natl Acad Sci USA 69:1384–1386.
47. Lesley J, English NM, Gal I, et al. 2002. Hyaluronan binding properties of a CD44 chimera containing the link module of TSG-6. J Biol Chem 277:26600–26608.
48. Lesley J, Gal I, Mahoney DJ, et al. 2004. TSG-6 modulates the interaction between hyaluronan and cell surface CD44. J Biol Chem 279:25745–25754.